Journal of Alloys and Compounds 509 (2011) 6476–6480

Contents lists available at ScienceDirect

Journal of Alloys and Compounds

journal homepage: www.elsevier.com/locate/jallcom

# Luminescence and energy transfer of $Mn^{2+}$ and $Tb^{3+}$ in $Y_3Al_5O_{12}$ phosphors

Zhongfei Mu[a,b], Yihua Hu[a,*], Haoyi Wu[a], Chujun Fu[a], Fengwen Kang[a]

[a] School of Physics and Optoelectronic Engineering, Guangdong University of Technology, Guangzhou 510006, PR China
[b] Experimental Teaching Department, Guangdong University of Technology, Guangzhou 510006, PR China

ARTICLE INFO

*Article history:*
Received 30 December 2010
Received in revised form 12 March 2011
Accepted 16 March 2011
Available online 23 March 2011

*Keywords:*
$Mn^{2+}$ and $Tb^{3+}$ codoped YAG phosphors
Luminescent properties
Energy transfer

ABSTRACT

$Mn^{2+}$ is an excellent luminescent ion with variable color from green, yellow to red in different hosts and has been widely utilized in recent years. The luminescent intensity of $Mn^{2+}$ in many hosts is so low that the correlative application is restricted. In the present paper, two methods, i.e. employing a charge compensator and introducing a sensitizer, were adopted to enhance the luminescence of $Mn^{2+}$ in $Y_3Al_5O_{12}$ (YAG). By employing $Si^{4+}$ as a charge compensator, the doping content of $Mn^{2+}$ ($x$) in $Y_3Mn_xAl_{5-2x}Si_xO_{12}$ can be lifted up to 0.4. $Mn^{2+}$ in YAG emits orange light in a broad band. The peak wavelength shifts from 586 to 593 nm with the increasing $x$. The luminescent intensity of $Mn^{2+}$ reaches its maximum when $x = 0.1$. Co-doping $Tb^{3+}$ into $Mn^{2+}$ doped YAG, the sensitization effect of $Tb^{3+}$ on $Mn^{2+}$ was observed clearly. The resonance energy transfer from $Tb^{3+}$ to $Mn^{2+}$ occurs because there is a well overlapping between emission spectrum of $Tb^{3+}$ and excitation spectrum of $Mn^{2+}$. A reasonable explanation for the sensitization effect of $Tb^{3+}$ on the luminescence of $Mn^{2+}$ was brought forward.



## 1. Introduction

Being an excellent luminescent ion with variable color from green, yellow to red in different hosts [1], $Mn^{2+}$ has obtained more and more comprehensive attention in recent years. Currently, $Mn^{2+}$ has been widely utilized in sulfides, phosphates, borates, aluminates, silicates [2–6], and so on, as an activator or sensitizer. The luminescence transition of $Mn^{2+}$ is parity and spin forbidden. Therefore, the luminescent intensity of $Mn^{2+}$ in many hosts is so low that the correlative application is restricted. There are two effective methods to be employed to enhance the luminescence of $Mn^{2+}$. One is increasing its doping content but the increment of doping content is restricted by many factors such as the radii of ions, chemical valence and attraction of elements, the bonding orbital of atoms, etc. The other is through the energy transfer from the other luminescent ions. Some rare earth ions such as $Ce^{3+}$ and $Eu^{2+}$ can be taken as the sensitizers of $Mn^{2+}$ because these ions can transfer the absorbed energy to $Mn^{2+}$ and enhance the luminescence of $Mn^{2+}$ [7–9].

$Y_3Al_5O_{12}$ (YAG) is a host with excellent structural compatibility. Inner $Y^{3+}$ and $Al^{3+}$ can be substituted by many kinds of cation with different sizes and valence in a certain extent. Many researchers investigated the effect of doping other ions on host structure and luminescence properties of usual luminescent ions [10–12]. However, few literatures reported the luminescence properties of $Mn^{2+}$ in YAG. The main reason for this is that the doping content is strongly restricted as a result of charge unbalance. A big doping content will bring new phases in phosphors which destroy the stable garnet structure. While a small doping content only brings weak luminescence which can nearly be inspected by the present instruments.

According to above depiction, it is very difficult to lift the luminescent intensity of $Mn^{2+}$. In this work, two methods are tried to enhance the luminescence of $Mn^{2+}$ in YAG. One is employing tetravalent cation ($Si^{4+}$) as a charge compensator to keep charge balance while the doping content of $Mn^{2+}$ in YAG is lifted up. The other is co-doping the other rare earth ions with the expectation that $Mn^{2+}$ has a better performance under the sensitization of the other ions. The emission bands of $Tb^{3+}$ in many hosts locate from 360 to 660 nm [13,14]. Some of them in ultraviolet (UV) or blue region usually approach or overlap the absorption bands of the other luminescent ions. For this reason, $Tb^{3+}$ is frequently selected as a sensitizer of the other luminescent ions. Especially, energy transfer from $Tb^{3+}$ to $Mn^{2+}$ has been observed in some hosts such as $LaMgAl_{11}O_{19}$ [15], $SrAl_{12}O_{29}$ [16], etc. It is expected and possible that $Tb^{3+}$ has a sensitization effect on $Mn^{2+}$ in YAG. To the best of our knowledge, there is no literature published which reported the sensitization effect of $Tb^{3+}$ on $Mn^{2+}$ in YAG up to now. In this work, a series of phosphors $Y_{3-y}Tb_yMn_xAl_{5-2x}Si_xO_{12}$ ($x = 0$, 0.05, 0.1, 0.15, 0.2, 0.3, 0.4; $y = 0.01$, 0.02, 0.03, 0.04, 0.05) were synthesized with traditional solid state reactions. The luminescence properties of $Mn^{2+}$ and $Tb^{3+}$ and the energy transfer from $Tb^{3+}$ to $Mn^{2+}$ were investigated. $Mn^{2+}$ can emit orange light in a broad band peaking from 586 to 593 nm. The energy transfer from $Tb^{3+}$

* Corresponding author. Tel.: +86 20 39322262; fax: +86 20 39322265.
*E-mail address:* huyh@gdut.edu.cn (Y. Hu).

0925-8388/$ – see front matter © 2011 Elsevier B.V. All rights reserved.
doi:10.1016/j.jallcom.2011.03.097

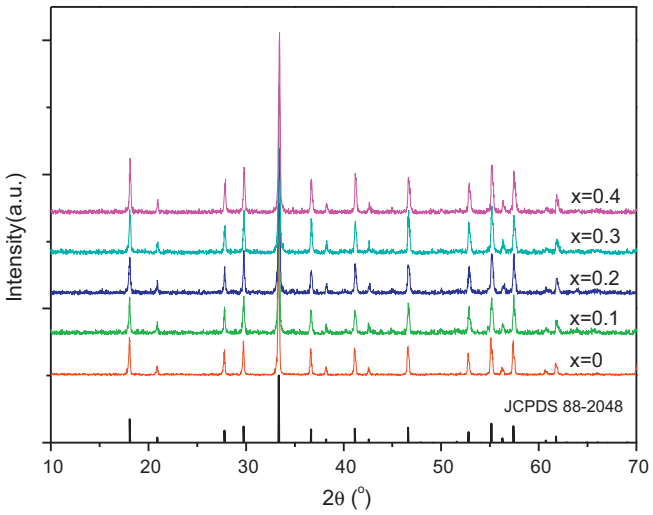


**Fig. 1.** The XRD patterns of $Mn^{2+}$ singly doped samples $Y_3Mn_xAl_{5-2x}Si_xO_{12}$.

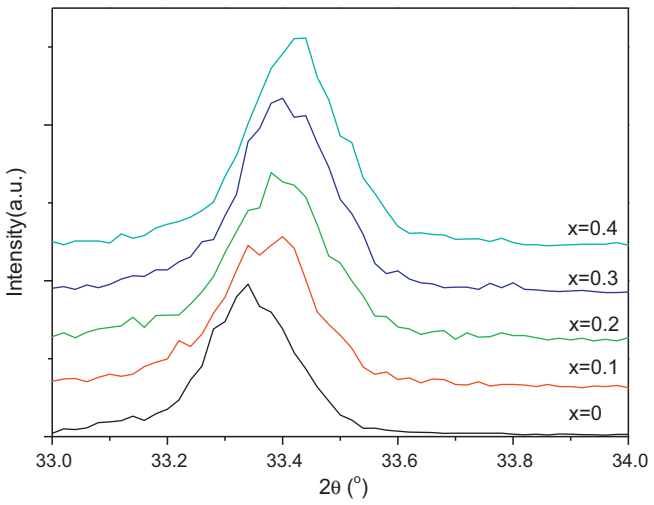


**Fig. 2.** The magnified part of the XRD patterns of $Mn^{2+}$ singly doped samples $Y_3Mn_xAl_{5-2x}Si_xO_{12}$.

to $Mn^{2+}$ enhanced the luminescence of $Mn^{2+}$ remarkably. The process and mechanism of energy transfer from $Tb^{3+}$ to $Mn^{2+}$ were also discussed. To be clear, in the following expressions the doping contents of $Mn^{2+}$ and $Tb^{3+}$ are abbreviated as italic $x$ and $y$, respectively.

## 2. Experimental

All the studied phosphors were synthesized with traditional solid state reactions. Firstly, raw materials $Y_2O_3$ (99.99%), $Al_2O_3$ (99.99%), $MnCO_3$ (99.0%), $SiO_2$ (99.0%) and $Tb_4O_7$ (99.99%) were accurately weighed according to the composition of $Y_{3-y}Tb_yMn_xAl_{5-2x}Si_xO_{12}$ ($x = 0, 0.05, 0.1, 0.15, 0.2, 0.3, 0.4$; $y = 0.01, 0.02, 0.03, 0.04, 0.05$). A small amount of $H_3BO_3$ was added into the raw materials as the flux. The weighed materials were put into an agate mortar and ground with an agate muller for 2 h in order to mix them thoroughly. Then they were heated up to 1550 °C with a constant heating rate (5 °C per minute) in a tubular furnace. A weak reducing atmosphere with $H_2$ (5%) and $N_2$ (95%) was employed in order to keep the valence of manganese and terbium to be +2 and +3, respectively. The samples were preserved at 1550 °C for 4 h, and then cooled naturally with the furnace. The cooled samples were ground again and filtered well before they were measured and analyzed.

The phase identification of prepared phosphors was carried out by a Beijing MSAL-XD-2 X-ray powder diffractometer (XRD) which worked with Cu Kα irradiation (λ = 0.15406 nm) at 36 kV tube voltage and 20 mA tube current. The excitation and emission spectra of the phosphors were measured with a Hitachi F-7000 Fluorescence Spectrophotometer. The work voltage of the spectrophotometer was fixed at 400 V and the width of the monochromator slits for both emission and excitation was fixed at 2.5 nm.

## 3. Results and discussion

### 3.1. Structure analysis

All the prepared phosphors were measured and analyzed by XRD. Comparing the XRD patterns of $Tb^{3+}$ singly doped samples with standard JCPDS cards by MDI jade 5.0 software, the main diffraction peaks are all consistent with JCPDS card No. 88-2048. Thus $Tb^{3+}$ singly doped samples can be indexed to YAG with single garnet structure. This indicates that a small amount of $Tb^{3+}$ does not change the phase structure of YAG significantly [17,18]. However, there is some difference among the XRD patterns when $Mn^{2+}$ is singly doped or co-doped into YAG. Fig. 1 presents the XRD patterns of $Mn^{2+}$ singly doped samples. They seem to be identical in Fig. 1. All of them can be indexed to YAG with single garnet structure. When these patterns are magnified (shown in Fig. 2), one can see clearly that with the increment of $x$, the diffraction peaks shift to higher angles. According to Bragg's equation, $2d\sin\theta = n\lambda$ (here $\lambda$ is the wavelength of employed X-ray, $n$ is the diffraction order, $\theta$ is the diffraction angle of the corresponding diffraction peak, $d$ is the interplanar distance of corresponding crystal plane), the movement of $2\theta$ to higher angles shows that the interplanar distance decreases gradually which subsequently results in the shrinkage of the crystal lattice. Hodges [19] pointed out that when $Mn^{2+}$ is doped into four kinds of garnet structures ($Y_3Al_5O_{12}$, $Lu_3Ga_5O_{12}$, $Lu_3Al_5O_{12}$, and $Y_3Ga_5O_{12}$), $Mn^{2+}$ can come into any of three kinds of sites. (Which are in the center of dodecahedron, octahedron and tetrahedron, respectively. In YAG, they are composed of $YO_8$, $AlO_6$ and $AlO_4$, respectively.) There are two obvious differences between our experiments and theirs. Co-doping content in our experiments is much bigger than theirs. $Si^{4+}$ was co-doped into YAG as a charge and volume compensator while the doping in their experiments was sole. The radii of the involved ions are as follows: $R(Y^{3+}{}_8) = 0.1019$ nm, $R(Al^{3+}{}_6) = 0.0535$ nm, $R(Al^{3+}{}_4) = 0.039$ nm, $R(Mn^{2+}{}_8) = 0.096$ nm, $R(Mn^{2+}{}_6) = 0.067$ nm, $R(Mn^{2+}{}_4) = 0.066$ nm, $R(Si^{4+}{}_4) = 0.026$ nm [20], the subscript here denotes the coordination number (CN) of the cation. According to the difference of radii among these ions and the ratio of raw materials, it is assumed that most of $Mn^{2+}$ comes into octahedron with CN = 6 to replace $Al^{3+}{}_6$, which makes the octahedron expand and $Si^{4+}$ comes into tetrahedron with CN = 4 to replace $Al^{3+}{}_4$, which makes the tetrahedron shrink. The results of XRD analysis indicate that with the increment of $x$, samples keep garnet structure all along. This proves that our assumption is right. With the increment of $x$, the shifting to higher angles of the main diffraction peaks indicates that the total effect of the co-doping of $Mn^{2+}$ and $Si^{4+}$ is making the crystal lattice shrink to a certain extent.

### 3.2. Luminescence of $Mn^{2+}$ in YAG

The excitation spectrum and emission spectrum of $Mn^{2+}$ singly doped sample $Y_3Mn_{0.1}Al_{4.8}Si_{0.1}O_{12}$ are shown in Fig. 3. Its excitation spectrum monitoring the emission at 587 nm is composed of the broad band in UV region and several absorption bands in violet-blue region. The broad band from 200 to 250 nm peaking at 221 nm looks a little instable with some line emissions. This might be related with the absorption of air to UV in this wave band. According to literatures [21–23], this broad band can be attributed to $Mn^{2+}$–$O^{2-}$ charge transfer (CT) transition. The emission spectra excited with 221 and 409 nm (the strongest excitation peak in violet-blue region) are shown in the right of Fig. 3. Their emission spectra are all broad bands peaking at 587 nm. According to the Tanabe–Sugano diagram of $3d^5$ configuration and some related lit-

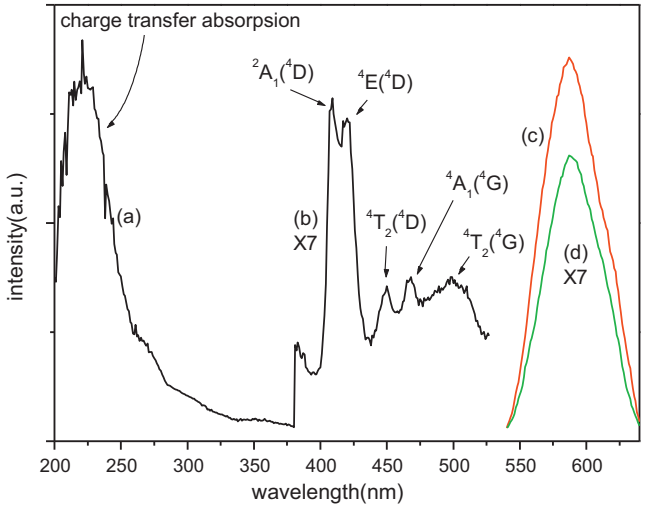


**Fig. 3.** The excitation spectrum and emission spectrum of $Mn^{2+}$ singly doped sample $Y_3Mn_{0.1}Al_{4.8}Si_{0.1}O_{12}$: (a) CT band monitoring 587 nm emission; (b) absorption bands in UV and violet-blue region monitoring 587 nm emission (7×); (c) emission spectrum excited with 221 nm; (d) emission spectrum excited with 409 nm (7×).

eratures [24–26], observed broad band emission can be ascribed to the transition of $Mn^{2+}$ from $^4T_1$ ($^4G$) to $^6A_1$ ($^6S$), and several absorption bands at 492, 467, 450, 419 and 409 nm can be assigned to the transition of $Mn^{2+}$ from the ground state $^6A_1$ ($^6S$) to the excited states $^4T_2$ ($^4G$), $^4A_1$ ($^4G$), $^4T_2$ ($^4D$), $^4E$ ($^4D$) and $^2A_1$ ($^4D$), respectively. This indicates that the sample can be excited efficiently by UV light and visible light in violet-blue region.

Fig. 4 presents the emission spectra of samples with different $x$ under the excitation of 409 nm. It is observed that all the emission spectra are in a broad band peaking around 590 nm, and the emission intensity increases firstly, decreases subsequently with the increasing $x$. When $x = 0.1$, the emission intensity reaches its maximum. The dependence of emission intensity of phosphors on $x$ is presented in the subgraph of Fig. 4. From that subgraph, it is also observed that the emission peak shifts to longer wavelength gradually (586, 587, 589, 590, 592 and 593 nm). The electron configuration of $Mn^{2+}$ is $[1s^2\ 2s^2\ 2p^6\ 3s^2\ 3p^6]\ 3d^5$. Five 3d electrons are in the outside of the other sublayers without any shield. Thus the energy level of these electrons is affected by crystalline field

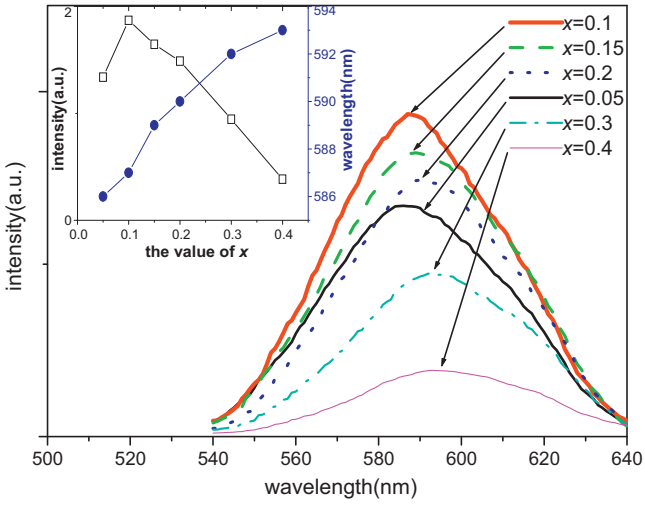


**Fig. 4.** The emission spectra of $Mn^{2+}$ singly doped samples $Y_3Mn_xAl_{5-2x}Si_xO_{12}$. The curve with hollow square symbols shows the functional relationship of the emission intensity with $x$, while the curve with solid circle symbols shows the functional relationship of the peak wavelength of emission spectra with $x$.

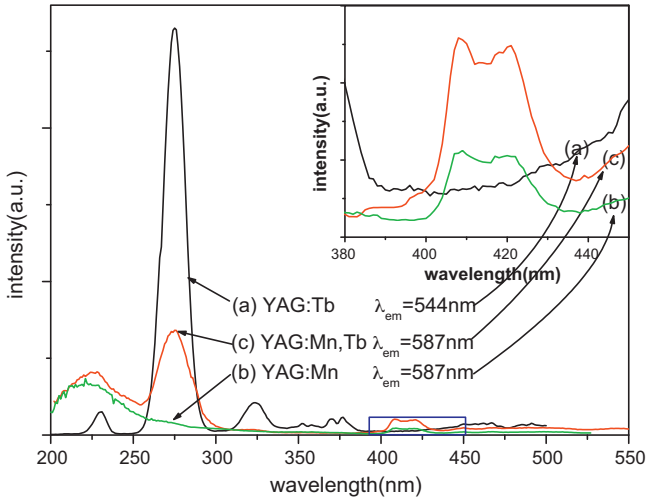


**Fig. 5.** The excitation spectra of samples $Y_{3-y}Tb^{3+}{}_yMn_xAl_{5-2x}Si_xO_{12}$: (a) the excitation spectrum of $Tb^{3+}$ singly doped samples $Y_{2.95}Tb_{0.05}Al_5O_{12}$ monitoring the emission at 544 nm; (b) the excitation spectrum of $Mn^{2+}$ singly doped sample $Y_3Mn_{0.1}Al_{4.8}Si_{0.1}O_{12}$ monitoring the emission at 587 nm; (c) the excitation spectrum of $Mn^{2+}$ and $Tb^{3+}$ co-doped sample $Y_{2.95}Tb_{0.05}Mn_{0.1}Al_{4.8}Si_{0.1}O_{12}$ monitoring the emission at 587 nm; the subgraph shows the magnified part surrounded by the rectangle in the main graph.

strongly. The results of XRD analysis indicate that the interplanar distance decreases gradually with the increasing $x$, which results in the decrement of the bond length. Consequently, the crystal field effects around $Mn^{2+}$ get stronger which enhances the splitting of $3d^5$ energy level. Thus the lowest energy of 3d energy level gets lower. This shows red shift in emission spectra macroscopically.

We also measured excitation spectra of samples with different $x$ monitoring the emission around 590 nm (not shown in the present paper). It is observed that the changing trend of the excitation intensity is similar to emission intensity, i.e. it increases firstly, decreases subsequently with the increasing $x$. When $x = 0.1$, the excitation intensity reaches its maximum. However, the position of excitation peaks does not show significant alternation.

### 3.3. Luminescence of $Tb^{3+}$ in YAG

Fig. 5(a) presents the excitation spectrum of $Tb^{3+}$ singly doped phosphor $Y_{2.95}Tb_{0.05}Al_5O_{12}$ monitoring the emission at 544 nm. There are three excitation bands corresponding to the transition from $4f^8$ to $4f^75d^1$ in this excitation spectrum. Their peak wavelength is 231, 275 and 324 nm, respectively. The weak excitation peaks in the region from 350 to 500 nm are due to the absorption of the forbidden f–f transitions of $Tb^{3+}$.

Fig. 6(a) presents the emission spectrum of $Tb^{3+}$ singly doped phosphor $Y_{2.95}Tb_{0.05}Al_5O_{12}$ excited with 275 nm. It can be separated into two groups. The first is the near-UV and blue emission below 480 nm, including several peaks at 385, 419 and 439 nm, ascribed to the $^5D_3$–$^7F_J$ ($J = 6, 5, 4$) transitions. The second is the green and red emission above 480 nm, including several peaks at 492, 544, 593 and 629 nm, corresponding to $^5D_4$–$^7F_J$ ($J = 6, 5, 4, 3$) transitions [17,18,27,28]. (For interpretation of the references to color in this text, the reader is referred to the web version of the article.)

### 3.4. The energy transfer from $Tb^{3+}$ to $Mn^{2+}$

Fig. 6(b) presents the emission spectrum of $Mn^{2+}$ singly doped sample excited with 221 nm, and Fig. 6(c) presents the emission spectrum of $Mn^{2+}$ and $Tb^{3+}$ co-doped sample excited with 275 nm. It can be pointed out that the emission spectra of co-doped sam-

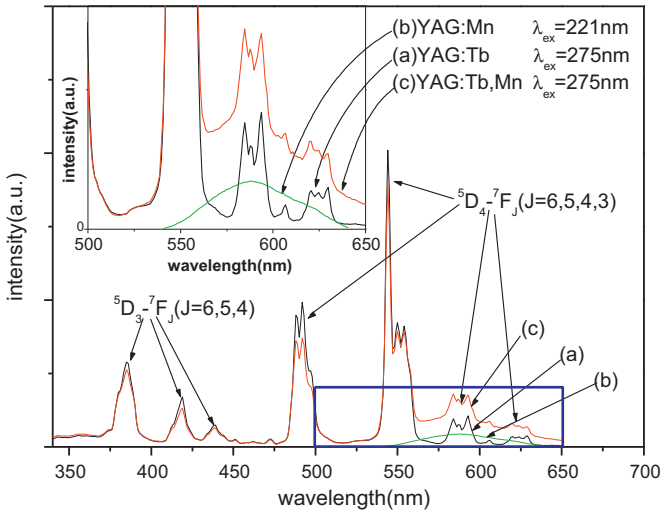


**Fig. 6.** The emission spectra of samples $Y_{3-y}Tb^{3+}{}_yMn_xAl_{5-2x}Si_xO_{12}$: (a) the emission spectrum of $Tb^{3+}$ singly doped samples $Y_{2.95}Tb_{0.05}Al_5O_{12}$ excited with 275 nm; (b) the emission spectrum of $Mn^{2+}$ singly doped sample $Y_3Mn_{0.1}Al_{4.8}Si_{0.1}O_{12}$ excited with 221 nm; (c) the emission spectrum of $Mn^{2+}$ and $Tb^{3+}$ co-doped sample $Y_{2.95}Tb_{0.05}Mn_{0.1}Al_{4.8}Si_{0.1}O_{12}$ excited with 275 nm; the subgraph shows the magnified part surrounded by the rectangle in the main graph.

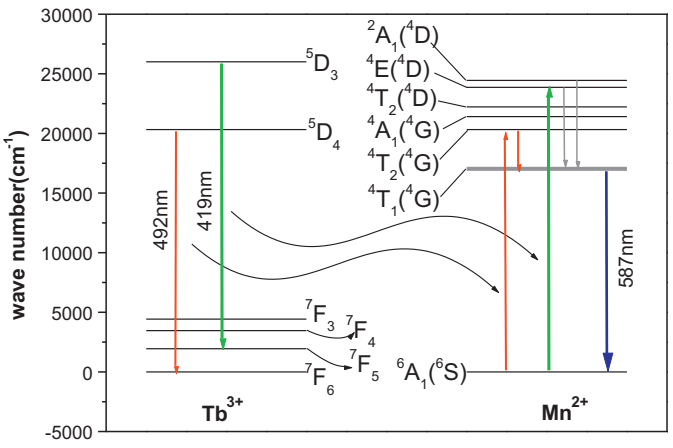


**Fig. 7.** Energy level diagrams for $Tb^{3+}$ and $Mn^{2+}$ in YAG. The red and green arrows indicate the transitions involving nonradiative energy transfer from $Tb^{3+}$ to $Mn^{2+}$. Blue arrow indicates the enhanced emission of $Mn^{2+}$. (For interpretation of the references to color in this figure legend, the reader is referred to the web version of the article.)

ple and $Tb^{3+}$ singly doped sample are similar where the emission of $Tb^{3+}$ is predominant. An interesting phenomenon revealed in Fig. 6 is that the part from 550 to 640 nm in the emission spectrum of co-doped sample is obviously composed of the emission in a broad band peaking at 587 nm of $Mn^{2+}$ and the emission peaks around 593 nm of $Tb^{3+}$. $Tb^{3+}$ can be efficiently excited with 275 nm. From the above analysis, in $Mn^{2+}$ singly doped samples, the 275 nm light has no obvious excitation effect on $Mn^{2+}$. However, in $Mn^{2+}$ and $Tb^{3+}$ co-doped sample, the emission in a broad band of $Mn^{2+}$ appears when the sample is excited with 275 nm. Obviously, the reason for the occurrence of this phenomenon is that $Tb^{3+}$ can transfer the absorbed energy to $Mn^{2+}$. An important observation which should be remarked is that orange emission peaking at 587 nm of $Mn^{2+}$ obtained from the excitation of 275 nm is remarkably higher than the one from the excitation of 221nm(the peak wavelength of the CT band in the excitation spectrum of $Mn^{2+}$). This indicates that the intensity of sensitized luminescence is not only much higher than the intensity from the intrinsic excitation (according to Fig. 3, the emission intensity excited with 409 nm is only about one tenth of the one excited with 221 nm, thus the emission spectrum excited with 409 nm was not shown in Fig. 6) but also higher than the emission intensity from the excitation of CT band.

From Fig. 6, it is also observed that the emission intensity near 492 nm and from 400 to 425 nm in the emission spectra of co-doped sample is a little lower than $Tb^{3+}$ singly doped sample. Clearly, the decrement here supplements the increment from 550 to 640 nm each other. This observation confirms that some $Tb^{3+}$ with higher energy transfer absorbed energy to $Mn^{2+}$. Subsequently, the emission intensity of $Tb^{3+}$ decreases while the luminescence of $Mn^{2+}$ is enhanced. Keeping $y = 0.05$ fixed, it is observed that the emission intensity of $Tb^{3+}$ in co-doped samples is always lower than $Tb^{3+}$ singly doped ones. But the emission intensity does not change with the increasing $x$ monotonically. The functional relationship of the emission intensity with $x$ is complicated and ambiguous, which needs further investigation. There are two aspects of reasons for this phenomenon. On one hand, the emission intensity of $Tb^{3+}$ is about ten times higher than the emission of $Mn^{2+}$. Thus only a small part of energy absorbed by the $Tb^{3+}$ in excited states is transferred to $Mn^{2+}$. The change of the emission intensity of $Tb^{3+}$ is too small to be measured credibly. On the other hand, the emission intensity of $Mn^{2+}$ in YAG does not increase with the increasing $x$ monotonically. When $x = 0.1$, the emission intensity reaches its maximum. Keeping $x = 0.1$ unchanged, we changed $y$ from 0.01, 0.02, 0.03, 0.04 to 0.05. It is observed that the luminescent intensity of $Mn^{2+}$ under the excitation of 275 nm increases with the increasing $y$. This further verifies the sensitization effect of $Tb^{3+}$ on $Mn^{2+}$ in YAG.

Fig. 5(b) and (c) presents the excitation spectra of $Mn^{2+}$ singly doped and $Mn^{2+}$, $Tb^{3+}$ co-doped samples monitoring the emission at 587 nm. From Fig. 5(c), when the luminescence of $Mn^{2+}$ in co-doped sample at 587 nm was monitored, a broad band with higher intensity peaking at 275 nm was obtained except for the broad band peaking at 221 nm and some absorption bands in the region from 380 nm to 550 nm. Clearly, the broad band peaking at 275 nm is from the excitation of co-doped $Tb^{3+}$. The intensity of the broad band peaking at 275 nm is much lower than the one obtained in the excitation spectrum of $Tb^{3+}$ singly doped sample. The reason for this is that the monitoring wavelength is not 544 but 587 nm. Magnifying the part surrounded by the rectangle in Fig. 5, we can see in the subgraph that the intensity of the excitation peaks from 380 to 450 nm in co-doped sample is higher than the one in $Mn^{2+}$ singly doped sample. This demonstrates that $Tb^{3+}$ can transfer absorbed energy to $Mn^{2+}$ in another way.

From Fig. 5, there are two excitation bands from 400 to 425 nm in the excitation spectrum of $Mn^{2+}$ singly doped sample which correspond to the transitions from ground state $^6A_1$ ($^6S$) to excited states $^4E$ ($^4D$) and $^2A_1$ ($^4D$). However, in the emission spectrum of $Tb^{3+}$ singly doped sample (Fig. 6) the emission band of the $Tb^{3+}$ from excited state $^5D_3$ to ground state $^7F_5$ just locates from 400 to 425 nm. The overlapping of these bands is very good. In addition, the excitation band peaking at 492 nm (Fig. 3), corresponding to the transition from ground state $^6A_1$ ($^6S$) to excited state $^4T_2$ ($^4G$), has a perfect overlapping with the emission band of the $^5D_4$–$^7F_6$ transition of $Tb^{3+}$ (Fig. 6). The perfect overlapping between the emission spectrum of $Tb^{3+}$ and the excitation spectrum of $Mn^{2+}$ brings convenience to the resonance energy transfer from $Tb^{3+}$ to $Mn^{2+}$. According to the theory of energy transfer developed by Dexter [29], the resonance energy transfer depends on the overlapping extent of the sensitizer's emission spectrum with the activator's excitation spectrum. In the process of the energy transfer from $Tb^{3+}$ to $Mn^{2+}$, $Tb^{3+}$ and $Mn^{2+}$ play the role of sensitizer and activator, respectively. Thus the energy transfer from the $Tb^{3+}$ to $Mn^{2+}$ depends on the overlapping extent of the emission bands of $Tb^{3+}$ and the absorption bands of $Mn^{2+}$. The energy transfer process may

be described as follows (Fig. 7). The energy that populates the $^5D_3$ energy level by direct absorption from ground state $^7F_5$ is transferred to $Mn^{2+}$ on the ground state $^6A_1$ by multipole interaction. Consequently, the energy level of a part of $Mn^{2+}$ is lifted from ground state $^6A_1$ to excited states $^2A_1$ or $^4E$. Subsequently, these $Mn^{2+}$ relax from higher excited states $^2A_1$ and $^4E$ to the lowest excited state $^4T_1$ by nonradiative relaxation. The energy that populates the $^5D_4$ energy level by direct absorption from ground state $^7F_6$ is transferred to $Mn^{2+}$ on the ground state $^6A_1$ by multipole interaction. The energy level of another part of $Mn^{2+}$ is lifted from ground state $^6A_1$ to excited state $^4T_2$. These $Mn^{2+}$ can also relax to the lowest excited state $^4T_1$ by nonradiative relaxation. The electron on the excited state $^4T_1$ returns to ground state $^6A_1$ by radiative transition. Simultaneously, a photon is emitted. The energy transfer from $Tb^{3+}$ to $Mn^{2+}$ increases the number of $Mn^{2+}$ which are lifted or relaxed to lowest excited state $^4T_1$. As a result, the red emission from $Mn^{2+}$ is enhanced significantly.

## 4. Conclusions

By employing $Si^{4+}$ as a charge compensator, the doping content of $Mn^{2+}$ in YAG was increased to a certain extent. On this basis, the structure and luminescence properties of $Mn^{2+}$ singly doped phosphor $Y_3Mn_xAl_{5-2x}Si_xO_{12}$ ($x = 0.05$, 0.1, 0.15, 0.2, 0.3, 0.4) were investigated. $Mn^{2+}$ in YAG emits orange light in a broad band. With the increment of the doping content, the emission peak shifts to longer wavelength and the emission intensity of phosphors increases firstly, decreases subsequently. The emission intensity reaches its maximum when $x = 0.1$. Two groups of emission peaks, corresponding to the optical transitions from excited states $^5D_3$ and $^5D_4$, to ground state $^7F_J$ ($J = 6$, 5, 4, 3), respectively, were observed in the emission spectra of $Tb^{3+}$ singly doped phosphors $Y_{3-y}Tb^{3+}{}_yAl_5O_{12}$ ($y = 0.01$, 0.02, 0.03, 0.04, 0.05). When $Tb^{3+}$ and $Mn^{2+}$ were co-doped into YAG, the obvious sensitization effect of $Tb^{3+}$ on $Mn^{2+}$ was observed which indicates that the energy transfer from $Tb^{3+}$ to $Mn^{2+}$ occurs. The reason for energy transfer from $Tb^{3+}$ to $Mn^{2+}$ is verified that there is a perfect overlapping between the emission spectrum of $Tb^{3+}$ and excitation spectrum of $Mn^{2+}$. The experiments and analysis in the present paper confirm that charge compensation and the sensitization of the other luminescent ions are two effective methods which can be utilized to enhance the luminescence of $Mn^{2+}$ in YAG.

## Acknowledgement

This work is supported by the National Natural Science Foundation of China (No. 21071034, No. 20871033).

## References

[1] X. Wang, D. Jia, W. Yen, J. Lumin. 102 (2003) 34.
[2] A.A. Bol, A. Meijerink, Phys. Rev. B. 58 (1998) 15997.
[3] Z. Yang, S. Ma, H. Yu, et al., J. Alloys Compd. 509 (2011) 76.
[4] L. Chen, Y. Zhao, X. An, et al., J. Alloys Compd. 494 (2010) 415.
[5] Y.H. Won, H.S. Jang, W.B. Im, et al., Appl. Phys. Lett. 89 (2006) 231909.
[6] X. Qu, L. Cao, W. Liu, et al., J. Alloys Compd. 494 (2010) 196.
[7] A. Nag, T.R.N. Kutty, Mater. Chem. Phys. 91 (2005) 524.
[8] X. Zhang, M. Gong, J. Alloys Compd. 509 (2011) 2850.
[9] Z. Hao, J. Zhang, X. Zhang, et al., Appl. Phys. Lett. 90 (2007) 261113.
[10] M. Kottaisamy, P. Thiyagarajan, J. Mishra, et al., Mater. Res. Bull. 43 (2008) 1657.
[11] J.D. Kmetec, T.S. Kubo, T.J. Kane, Opt. Lett. 19 (1994) 186.
[12] M. Gervais, S. LeFloch, N. Gautier, et al., Mater. Sci. Eng. B 45 (1997) 108.
[13] L. Yang, L. Zhou, X. Chen, et al., J. Alloys Compd. 509 (2011) 3866.
[14] F. Zhang, Y. Wang, J. Liu, J. Alloys Compd. 509 (2011) 3852.
[15] H. You, Y. Song, G. Jia, G. Hong, Opt. Mater. 31 (2008) 342.
[16] V.B. Mikhailik, Mater. Lett. 63 (2009) 803.
[17] G. Xia, S. Zhou, J. Zhang, et al., J. Alloys Compd. 421 (2006) 294.
[18] H.M.H. Fadlalla, C. Tang, A. Elsanousi, et al., J. Lumin. 129 (2009) 401.
[19] J.A. Hodges, J. Phys. Chem. Solids 35 (1974) 1385.
[20] R.D. Shannon, Acta Crystallogr. A: Found. Crystallogr. 32 (1976) 751.
[21] J. Lin, D.U. Sanger, M. Mennig, et al., Thin Solid Films 360 (2000) 39.
[22] J. Wang, S. Wang, Q. Su, J. Mater. Chem. 14 (2004) 2569.
[23] L. Lin, M. Yin, C. Shi, et al., J. Alloys Compd. 455 (2008) 327.
[24] V. Singh, R.P.S. Chakradhar, J.L. Rao, et al., J. Lumin. 128 (2008) 1474.
[25] C.J. Duan, A.C.A. Delsing, H.T. Hintzen, J. Lumin. 129 (2009) 645.
[26] Y. Zorenko, V. Gorbenko, T. Voznyak, et al., J. Lumin. 130 (2010) 380.
[27] R. Martinez-Martinez, A. Speghini, M. Bettinelli, et al., J. Lumin. 129 (2009) 1276.
[28] D. Hreniak, W. Strek, P. Mazur, et al., Opt. Mater. 26 (2004) 117.
[29] D.L. Dexter, J. Chem. Phys. 21 (1953) 836.